8th International Conference on Water Resources and Arid Environments (ICWRAE 8): 699-715
22-24 January 2019*, Riyadh, Saudi Arabia*

Amidoximated Polyacrylonitrile/Na-Y-zeolite Composite for the Sorptive Removal of Cu(II), Cd(II) and Pb(II) Metal Ions from Water

[1,2]K.Z. Elwakeel, [3]A.A. El-Bindary, [3]E.Y. Kouta and [4]Eric Guibal

[2]Chemistry Department, Faculty of Science, University of Jeddah, Jeddah, Saudi Arabia
[2]Environmental Science Department, Faculty of Science, Port-Said University, Port-Said, Egypt
[3]Chemistry Department, Faculty of Science, Damietta University, Damietta 34517, Egypt
[4]Ecole des mines d'Alθs, Centre des Matériaux des Mines d'Alθs (C2MA),
6, avenue de Claviθres, F-30319 Alθs cedex, France

Abstract: A composite material (PAN-Na-Y-zeolite) was prepared by polymerization of acrylonitrile in the presence of Na-Y zeolite. The composite was functionalized by amidoximation through the reaction of hydroxylamine on nitrile groups of the composite. The sorbent (APNa-Y-zeolite) was fully characterized by FTIR spectrometry, XRD diffraction, thermogravimetric analysis, scanning electron microscopy, zetametry and BET analysis. The sorption properties of APNa-Y-zeolite were investigated for the recovery of Cu(II), Cd(II) and Pb(II) from synthetic solutions before being tested for the purification of local tap water. Sorption properties were characterized through the study of pH effect, uptake kinetics, sorption isotherms. The pseudo-second order rate equation fitted well kinetic profiles. Sorption isotherms were modeled using the Langmuir, the Freundlich and the Sips equations. Thermodynamic parameters were evaluated through variation of temperature. While the sorption of Cu(II) and Cd(II) was endothermic, Pb(II) recovery was exothermic. Metal ions were successfully desorbed using 5 M HCl solutions. High concentrations of NaCl hardly alter sorption performance, contrary to humic acid that slightly reduces metal binding.

Key words: Heavy metal removal · Amidoximated PAN-Na-Y-zeolite composite · Sorption isotherms · Uptake kinetics · Metal desorption · Thermodynamic parameters.

INTRODUCTION

The contamination of water bodies by heavy metal discharge into the environment became a challenging issue for industry for the last decades. The international regulations on drinking water standard and the limit concentrations for discharge into the environment are becoming stricter [1]. The persistence and toxicity of these metals and their bioaccumulation at the different steps of the food chain may explain that the regulation laws are requiring very low metal standards [2, 3]. Metals like copper, cadmium and lead are presentative of these hazardous metals that are strongly controlled in terms of health and environmental impact [4]. They are abundantly used in industry, including mining, metallurgy [5, 6], electroplating [7, 8], textile, ceramics, batteries [9-11], etc.

Numerous processes have been designed for the removal of heavy metal ions from wastewaters. The application of these processes depends on the objective, including environmental objective for decreasing the concentration of hazardous contaminants and the recovery of valuable metals that require high concentration effect and selective separation. Precipitation process allows easy removal of metal ions but produces huge amounts of contaminated sludge. The technique is generally poorly selective [12]; although some specific processes may contribute to separate target metals [8]. Solvent extraction [13, 14] is a very efficient method for recovering metal ions in effluents containing relatively high metal concentrations (usually higher than several hundred of mg L^{-1}); however, the loss of toxic and expensive extractant by dissolving in water and physical dispersion limits the application to valuable metals and

Corresponding Author: K.Z. Elwakeel, Chemistry Department, Faculty of Science, University of Jeddah, Jeddah, Saudi Arabia. E-mail: khalid_elwakeel@yahoo.com.

high concentration effluents. This technique is thus poorly competitive for low metal concentration (below 50-100 mg L^{-1}). For dilute solutions, sorption processes are generally more interesting, using, for example: ion-exchange and chelating resin [11], extractant impregnated resin [15-17], inorganic sorbents [18-20], activated carbon [21, 22], carbon-based/polymer composites [23], biosorbents [24-28]. Zeolite materials are three-dimensional alumino-silicate frameworks constituted of tetrahedral SiO_4 and AlO_4arrangements. they have a global anionic surface, which, in turn, is neutralized by an external cationic framework (constituted of Na^+, Ca^{2+} or Mg^{2+});. This his opens the way to the binding of heavy metal cations by ion-exchange on natural zeolites[29]. Zeolite Y is an emblematic example of material having good textural properties [30] and sufficient availability for developing large-scale applications. However, the sorption properties are generally relatively weak and it is necessary functionalizing their surface for improving metal recovery.

Polymers offer many advantages for the elaboration of sorbents including the possibility to manage (a) the form and porosity of the sorbents, (b) the readily functionalization of the surfaces by grafting new reactive groups having higher affinity or selectivity for target metals. However, it may be interesting combining the advantages of these synthetic polymers with the high specific surface area of zeolite and other mesoporous materials: the deposition of the polymer at the surface of the porous support (through on-surface polymerization) may improve mechanical properties, textural characteristics and then mass transfer performance of composite materials,which can be used for metal binding[31, 32].The polymerization of poly(acrylonitrile) at the surface of Na-Y-zeolite allows synthesizing composite supports that can be further functionalized by reaction with an alkaline solution of hydroxylamine hydrochloride to convert nitrile groups into amidoxime groups [33-35]. Amidoxime-based sorbents have been abundantly studied for the recovery of uranium from aqueous solutions [33, 36-39], including sea water[40-46]. However, though less documented, amidoxime-based sorbents have also been investigated for heavy metal recovery [39, 47-52].

This study describes the synthesis of a sorbent based on amidoxime functionalized PAN/Na-Y-zeolite. The material is characterized by scanning electron microscopy (SEM), X-ray diffraction, Brunauer-Emmett-Teller (BET) analysis, thermogravimetric analysis, FTIR spectroscopy and zetametry. In a second step, the sorption properties of the sorbent are evaluated through the study of pH effect, uptake kinetics, sorption isotherms. The thermodynamic parameters are also evaluated. Metal desorption and sorbent recycling are also tested. The sorption properties are evaluated in the presence of NaCl and humic acid, before testing the sorption properties in metal-spiked tap water.

MATERIALS AND METHODS

Materials: Acrylonitrile (AN) was supplied by Fluka AG (Buchs, Switzerland). Na-Y-zeolite, hydroxylamine hydrochloride, methanol, potassium persulfate were purchased from Loba Feinchemie GmbH (Fischamend, Austria). Humic acid was obtained from Sigma-Aldrich Chemie GmbH (Munich, Germany). All reagents were analytical grade. Cu(II), Pb(II) and Cd(II) standard solutions (1000 mg L^{-1}) were used as stock solutions for preparing metal ions solutions; working solution were prepared by dilution just prior experimental tests. Tap water was collected on the municipal water network managed by Damietta Water Company (Damietta, Egypt).

Copolymerization Procedure for PAN/Na-Y-zeolite Synthesis: For the synthesis of the composite the precursors (acrylonitrile monomer and Na-Y-zeolite) were mixed with 50 mL of demineralized water: theAN/zeolite mass ratio was varied according the values 1:1, 1:2 and 1:3 (i.e.: 20 g of AN and 20 g, 40 g or 60 g of Na-Y-zeolite). A fixed amount (i.e., 0.1 g of potassium persulfate) was added as the initiator of polymerization reaction. The reaction was performed in a reactor equipped with a mechanical stirrer with a temperature controlled to 70 °C. After 4 h of reaction the solid (PAN-Na-Y-zeolite composite) was recovered by filtration, washed up with ethanol and air-dried. REFERENCE.

Functionalization of Composite with Amidoxime Groups: The functionalization of the composite was performed by reaction of nitrile groups on PAN-Na-Y-zeolite using hydroxylamine [53]. First, hydroxylamine hydrochloride (42.1 g) was dissolved in 300 mL a methanol/water mixture (5:1, volume ratio); the solution was neutralized with NaOH to pH 10. The methanol/water ratio was controlled as close as possible to 5:1. Sodium chloride precipitate was removed by filtration. In a second step, the PAN-Na-Y-zeolite composite was dropped into the hydroxylamine solution. The reactor was equipped with a condenser and a mechanical stirrer. After 2 h of reaction at 70 °C, the sorbent was removed by filtration, washed up several

times with methanol/water solution (4:1, volume ratio), before being treated with 200 mL of a 0.1 M HCl/methanol solution for 15 min. Finally, the sorbent was rinsed several times with a methanol/water solution (4:1, volume ratio) and dried at 50 °C (till constant weight). Scheme S1 shows the reaction pathway and the suggested structure of the sorbent (see Supplementary Material).

Characterization of the Sorbent: The morphology of sorbent particles was characterized using a scanning electron microscope (JEOL-JSM-6510 LV, Jeol, Tokyo, Japan). The textural properties of the sorbent (BET surface, pore volume and pore size) were characterized using a Quantachrome NOVA 3200e surface area and pore analyzer; data analysis was performed using NovaWin software (v11.0)(Quantachrome Instruments, Boynton Beach, FL, USA). X-ray diffraction analysis was performed using a Shimadzu XRD-6000 diffractometer(Shimadzu Corporation, Tokyo, Japan) in the range 2θ: 5-80 °, with Cu $K_á$ radiation (λ=1.540598 Å). Thermogravimetric analysis was operated on Shimadzu TGA-50 thermogravimetric analyzer (Shimadzu Corporation, Tokyo, Japan): analysis was performed under N_2 atmosphere with a temperature ramp of 10 °C min^{-1}, in the range 20-999 °C. FTIR analysis was carried out using a JASCO-FT/IR-4100 spectrometer (Jasco, Easton, MD, USA): the finely grinded samples were incorporated into KBr discs prior to analysis in the wavenumber range 400-4000 cm^{-1}. The zeta potential of the sorbent was measured using a Nano Zeta Sizer (Nano-ZS Malvern Instruments Ltd., London, United Kingdom) at various pHs from 1 to 8. A 0.01 g of the sorbent was mixed with 50 mL of 0.1 M KCl. The suspension was then adjusted to the specified pH and kept under stirring for 15 min. After conditioning, the suspension was left for another 15 min for settling before measurements.

The pH measurements were performed on an Orion Russell RL060P pH meter (Thermo Fisher Scientific, Beverly, MA, USA).

Sorption Experiments: The influence of H on metal sorption was investigated in batch system by contact of 25 mL (V) of the metal solution (initial metal concentration, C_0: 10 mg L^{-1}) with 25 mg (m, dry weight) of sorbent. Experiments were performed at room temperature (i.e., 25 ± 1 °C);with initial pH varying between 1 and 9 (pHcontrolled with 0.01-0.1 M HCl or 0.01-0.1 M NaOH solutions). The suspension was maintained under agitation at an agitation speed of 210 rpm (reciprocal shaker FINEPCR SH30L, FINEPCR, Gyeonggi-do, Korea) for 90 min. The contact time was set after preliminary kinetic tests that show that the equilibrium was reached within 90 min. The pH was not controlled during the sorption but the final pH was systematically monitored. The residual metal concentration (C_{eq}, mg L^{-1} or mmol L^{-1}) in the filtrate (pore size of filtration membrane: 1 µm) was determined by flame atomic absorption spectrophotometry (AAS, VARIAN AA240FS, Varian, now Agilent, Santa Clara, CA, USA).

Sorption isotherms were obtained by contact of 25 mg of sorbent with 25 mL of metal-containing solutions (C_0 varying between 5 and 100 mg L^{-1}) at pH initially set to 4 at room temperature (i.e., 25 ± 1 °C);. The suspension was maintained under agitation for 90 min. The residual metal concentration was determined by AAS and the sorption capacity (q, mg g^{-1} or mmol g^{-1}) was calculated by the mass balance equation: $q= (C_0-C_{eq})\times V/m$.

Thermodynamic studies were performed by contact of 25 mg of sorbent with 25 mL of metal ion solution (C_0: 40 mg L^{-1}) at initial pH 4 for Cu(II) and Cd(II) and at initial pH 3 for Pb(II). The suspension was maintained under agitation at constant temperature for 90 min; the temperature was varied between 25 °C and 50 °C. Residual concentration was determined after filtration and the sorption capacity was calculated by the mass balance equation.

Uptake kinetics were obtained by contact of 250 mg of sorbent with 250 mL of metal ion solution (initial pH 4; C_0: 40 mg L^{-1}) at room temperature (i.e., 25 ± 1 °C); agitation speed was set to 210 rpm. Samples (4 mL-volume) were withdrawn at fixed contact times and the metal concentration was analyzed by AAS, after filtration. The sorption capacity was determined as a function of time using the mass balance equation taking into account the decrement of the volume of the solution (with successive samples) according to:

$$q^{(t)} = \sum_{i=1}^{n} \frac{(C(t)_{(i-1)} - C(t)_{(i)}) \times V^{(t)}{}_{(i-1)}}{m} \quad (1)$$

where $C(t)_{(i)}$ (mgL^{-1}) is the Cu(II), Cd(II) or Pb(II) concentration of the withdrawn sample number i at time t and $C(t)_{(0)}= C_0$, $V(t)_{(i)}$(mL) is the volume of the solution in the flask at sample number i and time t and m is the mass of the sorbent in the flask. Here $V(t)_{(i)}$-$V(t)_{(i-1)}$ equals 4 mL (the sample volume).

Complementary experiments were performed to investigate the direct effect of sorbent dosage on metal sorption performance. Experiments were performed at

Table 1: Uptake kinetics – Modeling with the PFORE and PSORE

		PFORE				PSORE			
Metal	$q_{eq,exp.}$ (mmol g^{-1})	$q_{eq,1}$ (mmol g^{-1})	k_1 (min^{-1})	Est. Var. × 10^4	R^2	$q_{eq,2}$ (mmol g^{-1})	k_2 (g $mmol^{-1}$ min^{-1})	Est. Var. × 10^5	R^2
Cu(II)	0.552	0.0.536	0.175	3.22	0.985	0.561	0.492	19.8	0.991
Cd(II)	0.362	0.351	0.205	1.13	0.978	0.365	0.932	8.93	0.990
Pb(II)	0.171	0.168	0.236	0.39	0.980	0.173	2.411	0.16	0.999

Table 2: Sorption isotherms – Modeling with the Langmuir, the Freundlich and the Sips equations

		Langmuir				Freundlich				Sips				
Metal	$q_{m,exp.}$ (mmol g^{-1})	$q_{mL,exp.}$ (mmol g^{-1})	b_L (L $mmol^{-1}$)	EV ×10^3	R^2	k_F	n	EV×10^3	R^2	$q_{mS,exp.}$ (mmol g^{-1})	b_S (L $mmol^{-1}$)	n	EV ×10^3	R^2
Cu(II)	0.758	0.694	56.16	2.9	0.956	0.816	4.20	3.2	0.950	0.856	6.098	1.75	1.3	0.981
Cd(II)	0.378	0.376	91.96	5.3	0.909	0.423	8.18	0.26	0.907	0.423	12.51	1.82	0.19	0.912
Pb(II)	0.358	0.354	186.8	0.98	0.957	0.467	5.40	1.55	0.906	0.405	15.96	1.77	0.32	0.981

Table 3: Sorbent recycling: desorption (DE, %) and regeneration (RE, %) efficiencies for 5 successive sorption/desorption cycles

	Cu(II)		Cd(II)		Pb(II)	
Cycle #	DE (%)	RE (%)	DE (%)	RE (%)	DE (%)	RE (%)
1	94.9	n.a.	92.9	n.a.	91.9	n.a.
2	93.6	94.1	92.3	91.6	90.8	92.1
3	93.1	92.4	90.1	89.4	90.2	91.3
4	92.1	90.6	91.2	90.6	90.4	90.8
5	90.9	90.1	90.1	90.2	89.8	90.3

n.a.: not applicable

room temperature (i.e., 25 ± 1 °C) by contactof given amounts of sorbent with metal solutions at initial pH 4.0 (C_0: 40 mg L^{-1}), under agitation for 90 min. The composition of the solution may affect metal sorption; in order to evaluate this parameter, a series of experiment was performed under similar conditions with increasing amounts of NaCl (effect of ionic strength) and humic acid (effect of soil extract). Twenty mL of solution (C_0: 40 mg L^{-1}) at pH 4.0 and at 25 °C were mixed for 90 min with 25 mg of sorbent (with appropriate addition of NaCl and humic acid).

The feasibility of metal desorption was tested by contact of the Cu-loaded sorbent with 20 mL of 0.1-0.6 M HCl solution for 60 min. After filtration, the sorbent was carefully washed with demineralized water for reuse in a second run, while the metal concentration was evaluated in the filtrate by AAS and the mass balance equation was used for calculating the desorption % (DE, %) and regeneration efficiency (RE,%):

$$DE(\%) = \frac{Amount\ of\ sorbed\ metal\ (mg)}{Amount\ of\ sorbed\ metal\ (mg)\ at\ run\ n} \times 100 \quad (2)$$

$$RE(\%) = \frac{Amount\ of\ sorbed\ metal\ (mg)\ at\ run\ (n+1)}{Amount\ of\ sorbed\ metal\ (mg)\ at\ run\ n} \times 100 \quad (3)$$

Similar experiments were performed on Cd(II) and Pb(II) using exactly the same experimental conditions. The experimental conditions for both sorption and desorption steps were used for comparing desorption and regeneration efficiencies for the recovery of the three metal ions for 5 successive cycles.

Note: Full experimental conditions are systematically reported in the caption of the figures and tables. Supplementary Material gives a reminder on the main concepts involved in the modeling of uptake kinetics and sorption isotherms and the relevant models (Tables S1 and S2).

Testing on Tap Water: Specific experimental conditions have been used for testing the potential of this sorbent for water purification for tap water delivered by the local water supply company (i.e., Damietta water Company, Egypt). The chemical composition of this tap water is reported in Table S3 (see Supplementary Material). This tap water was spiked with variable amounts of Cu(II), Cd(II) and Pb(II) metal ions in order to evaluate the performance of this sorbent for this specific application of water purification (low metal concentration range). The sorption test was performed by contact of 25 mg of sorbent with 25 mL of the water sample at natural pH (without adjustment). Sorption performance was calculated by mass balance after 90 min of contact and filtration.

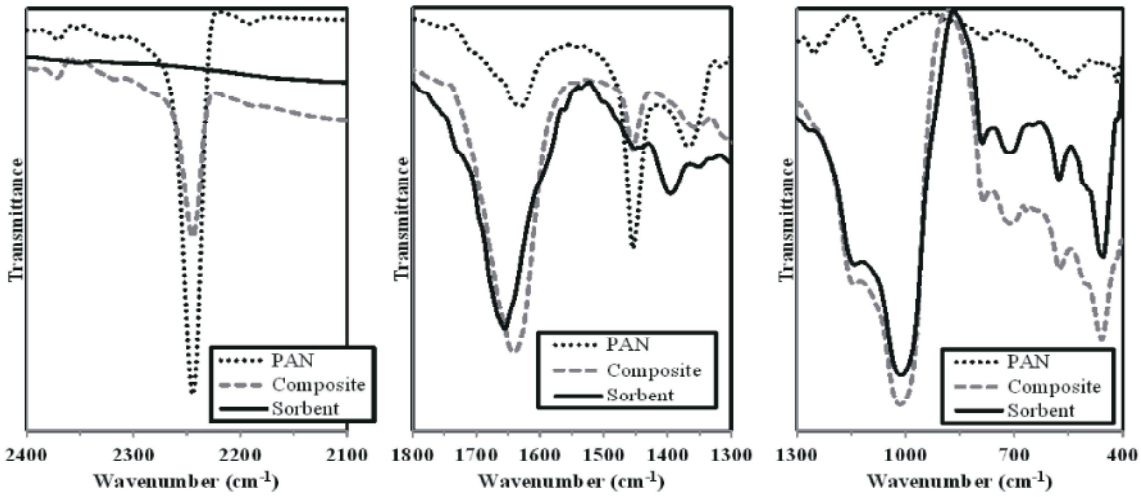

Fig. 1: FTIR spectra of PAN, PAN/Na-Y-zeolite composite and amidoxime derivative of composite (sorbent).

RESULTS AND DISCUSSION

Sorbent Characterization

Morphology and Textural Properties: Figure S1 (see Supplementary Material) shows the SEM micrographs of the sorbent before and after Cu(II) sorption. The amidoximated PAN/Na-Y-zeolite composite is characterized by relatively homogeneous zeolite particles (in the range 1-2 μm); though some clusters of particles can be identified. The particles are very similar to those reported by Jiao *et al*. [60]: they are characterized as irregular rectangular cubes. After copper binding the aspect of the surface slightly changes: although crystalline particles can still be observed, Cu(II) coverage leads to smoothed surfaces; the aggregation is reinforced by formation of larger clusters.

The textural analysis of the sorbent was performed by BET measurements using different calculation methods. The multipoint BET method gives a specific surface area of 66.1 $m^2 g^{-1}$ (close to the values obtained by the de Boer t-method external surface method; i.e., 6.62 $m^2 g^{-1}$). Other methods show a greater dispersion: 50.6, 87.7 and 89.3 $m^2 g^{-1}$ for the DFT cumulative surface area, Barret-Joyner-Halada method of cumulative desorption surface area and Denavit-Hartenberg parameters method, respectively (72.0 ± 14.6 $m^2 g^{-1}$). Similar dispersions in data are observed for the calculation of pore volume and pore size: 0.108 ± 0.008$cm^3 g^{-1}$and 27.4 ± 7.7 Å. These values are far from the expected values of Na-Y-zeolite: 797 $m^2 g^{-1}$ for the specific surface area and 0.40 $cm^3 g^{-1}$ for the pore volume (0.5 $cm^3 g^{-1}$ corresponding to the microporous volume) [60]; actually the textural properties of the Na-Y zeolite used in this study are much lower: the specific surface area was measured to 199.5 $m^2 g^{-1}$ (up to 163.4 and 268.4 $m^2 g^{-1}$ with the BJH and DH methods, respectively). The pore volume was measured to 0.2 $cm^3 g^{-1}$.This drastic decrease in the specific surface area is directly related to both the coating of the particles with PAN layer and aggregation phenomena of zeolite particles (also observed by SEM analysis). It is noteworthy that the PAN-Na-Y zeolite has textural properties close to those observed for the amidoximated sorbent (i.e., 62.5 $m^2 g^{-1}$ for the specific surface area and 0.111 $cm^3 g^{-1}$ for the pore volume): the chemical modification hardly affects the textural properties of the PAN-decorated zeolite.

X-ray Diffraction Analysis: The crystalline structure of the material was analyzed by XRD analysis (in the range 2θ: 5-80 degree): Figure S2a (see Supplementary Material) shows the XRD patterns of the composite (PAN-Na-Y-zeolite) while Figure S2b shows the material after chemical modification (amidoxime formation). The chemical modification of the composite hardly changes the crystalline structure of the material; the XRD patterns are very close to the XRD patterns of Na-Y-zeolite and its chemically derivative [60]. The presence of the organic phase is identified by the irregular wavy baseline (in the range 2θ: 15-40 degree).,The size of the crystallites (D_{DS}), calculated by the Debye-Scherrer equation (see Supplementary Material, Figure S2), was calculated for different peaks on the XRD patterns: in the case of PAN/Na-Y-zeolite the crystal size is 447 ± 16 Å, while after chemical modification the size of crystallites slightly increases to 506.2 ± 51.4 Å.

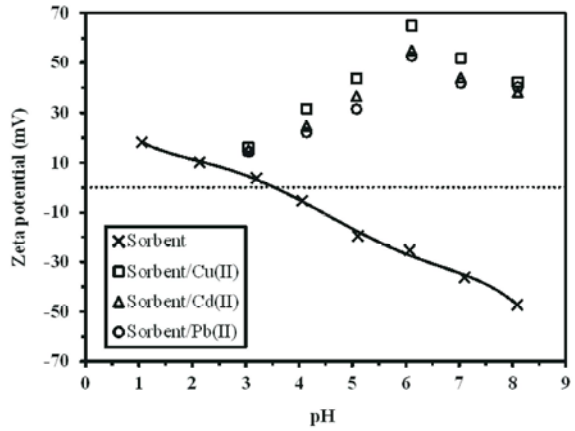

Fig. 2: Zeta potential of sorbent for pH_{ZPC} determination and for sorbent loaded with Cu(II), Cd(II) and Pb(II) (sorption capacities: 45.2 mg Cu g^{-1}, 42.5 mg Cd g^{-1} and 74.3 mg Pb g^{-1}, for metal loaded sorbent pH below was not analyzed due to possible phenomena of metal desorption).

Thermogravimetric Analysis: The thermogram of the sorbent shows different steps in the thermal degradation (Figure S3, see Supplementary Material). The total weight loss reaches 54% at 1000 °C. This residual amount corresponds to the dry zeolite fraction in the sorbent. The thermogram shows three main waves of weight loss, which are clearly identified on the DTG (derivative of TGA curve). Around 100 °C the weight loss corresponds to water release (about 15% of total weight): the small shoulder appearing at 80 °C probably means that water release is occurring in two steps: the water fraction associated to the polymer layer and the water incorporated in the zeolite. The second weight loss occurs close to 265 °C and counts for 15% of total weight. This is consistent with the thermo-gravimetric analysis of a composite associating PAN and Zn-Al layered double hydroxide composite [61]. Barik et al. observed the decomposition of nitrile groups of PAN in the range 230-315 °C. The last step in the weight loss corresponded to the degradation of ethylene-based chain of PAN in the range 315-620 °C. With amidoximated-PAN/Na-Y-zeolite the final degradation takes place in the range 450-600 °C (DTG peak close to 490 °C) and corresponds to a weight loss of about 24%. The DTG peak shows a weak shoulder close to 545 °C; this may be due to different profiles for the thermal degradation of ethylene-based groups and amidoxime groups. This is consistent with results reported by Zahri et al. [62] for amidoximated-PAN polymer.

FTIR Analysis: FTIR spectrometry analysis was performed on PAN, as the reference material, PAN/Na-Y-zeolite composite and the sorbent, after amidoximation of the composite (Figure 1 and Figure S4, see Supplementary Material). Different windows have been considered for highlighting the most significant differences observed during polymer modification.The large and poorly-resolved band in the range 3100-3700 cm^{-1} can be assigned to the overlapping of O-H and C-N stretching vibrations [62] (Figure S4). The peak at 2244 cm^{-1} (stretching vibration of CN groups), present on both PAN and composite materials, disappears after amidoximation: the nitrile groups of PAN are completely substituted by amidoxide groups [33] (at least below the detection limits). The other usual band which is representative of the stretching vibration of CN groups at 1072 cm^{-1} is masked by the large band appearing between 900-1200 cm^{-1}; which is associated to the tetrahedral arrangement of zeolite [63] and centered around 1010 cm^{-1}. The band at 1635-1640 cm^{-1} appearing on composite material is attributed to Na-Y-zeolite structure [64]. After amidoximation the peak is shifted toward higher wavenumber (i.e., close to 1655 cm^{-1}): this shifted peak corresponds to hydroxyimine (characteristics of amidoxime functional group) [65] and/or the overlapping of stretching vibrations of C=N and C=O vibrations [62]. A new band is appearing at 1398 cm^{-1} after chemical modification of PAN; this band is also observed for the amidoximation of PAN fibers [46]. The band at 1456 cm^{-1}, which is assigned to CH_2 groups, is decreased after chemical modification. The band at 456 cm^{-1} that appears on composite and amidoximated composite is directly associated to the tetrahedral vibration [63].FTIR spectra confirm the structure of PAN-deposited on Na-Y-zeolite support and highly converted to its amidoxime form.

Determination of pH_{ZPC}: Zetameter measurements (Figure 2) show that the pH_{ZPC} is close to 3.4. This is of the same order of magnitude than the pH_{ZPC} reported for amidoxime modified lignocellulosic material (close to 4) [66] or for amidoximated acrylonitrile/itaconic copolymers (close to 3.9) [67]. For amidoximated graphene oxide the pH_{ZPC} was found close to 4.2. After anchoring PAN on MCM-41 particles, Bayramoglu and Arica [36]proceeded to the amidoximation of composite material and they found that the pH_{ZPC} of pristine MCM-41 increased from 2 to 10.5.The amidoximation of PAN fibers increased the pH_{ZPC} from 3.7to 5.8 [68]. In the case of amidoximated

Table 4: Sorption performances for the removal of Cu(II), Cd(II) and Pb(II) from spiked tap water

Metal ion	C_0 (mg L^{-1})	C_{eq} (mg L^{-1})	Removal efficiency (%)	q (mol g^{-1})
Cu(II)	5.22	0.96	81.6	67.0
	2.77	0.33	88.1	38.4
Cd(II)	4.30	0.80	81.4	31.1
	3.00	0.60	80.0	21.4
Pb(II)	4.03	0.62	84.6	16.5
	3.16	0.46	85.4	13.0

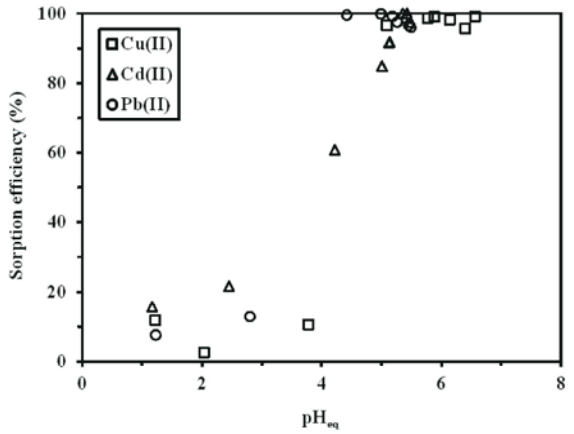

Fig. 3: pH effect on sorption efficiency (sorbent dosage, SD: 1 g L^{-1}; C_0: 10 mg L^{-1}; agitation time: 90 min, temperature: 25 ± 1 °C).

bacterial cellulose a much higher pH_{ZPC} was reported, close to 6.6 [69]. The pH_{ZPC}increase was even more marked in the case of the amidoximation of PEI-modified microalgae biomass (from 3.8 to 10) [37].

This means that at pH lower than 3 the sorbent will have a cationic charge with proton binding on amine groups. The deprotonation of hydroxyl group at higher pH may lead to an anionic charge of material surface.

After metal sorption (at a level of metal concentration close to the maximum sorption capacity) the surface charge of the materials is systematically positive and increases between pH 3 and pH 6; above pH 6, the surface charge remains positive but tends to decrease, regardless of the metal. Below pH 3, the possible desorption of the metal may interfere with the analysis of charge and the data have not been collected. The positive charge means that the sorption mechanism is not a strict charge neutralization mechanism.

Sorption Properties

Influence of Zeolite Fraction in the Composite: A preliminary test was performed to evaluate the impact of the zeolite content in the sorbent on sorption properties. Figure S5 and Table S4 (see Supplementary Material) show that increasing the mass fraction of the zeolite in the sorbent (i.e., decreasing the PAN:Na-Y-zeolite mass fraction) decreases the sorption capacity for the different metal ions. Obviously, decreasing the amount of the reactive polymer decreases the efficiency of the sorbent. It is noteworthy that this effect depends on the type of metal ion; the limiting effect decreases according the sequence: Cd(II) > Cu(II) > Pb(II). The expected benefit of zeolite in the composite consists of the increase in the specific surface area. As a consequence, the incorporation of zeolite is expected to increase uptake kinetics.However, the effective proportion should also take into account the decrease in the density of reactive groups in the composite material. Adjusting the mass fraction PAN:Na-Y-zeolite to 0.5 appears a good compromise. This value was selected for the complete study of sorption performance.

Influence of pH and Binding Mechanism: The pH may change the surface charge of the sorbent but also the speciation of metal ions in the solution; these two phenomena influence metal binding. The formation of hydrolyzed species may lead in some cases to metal precipitation but can also change the size and the charge of metal species. which, in turn, may affect their affinity for reactive groups on the sorbent. Figure 3 shows the effect of pH on sorption efficiency. The sorption efficiency remains below 20% when pH is below 4: metal ions are present as free metal cations (concentration ranging between 0.05 and 0.16 mM). The strong competition of protons may explain the weak sorption of metal cations. This is consistent with the value of pH_{ZPC} of the sorbent, which is close to 3.4: the surface of the sorbent is positively charged and limits the binding of metal cations (which are rejected). Above pH 3.6, the surface charge becomes negative and the repulsion effect progressively decreases [70]. Amine groups being deprotonated can bind metal cations; the deprotonation of OH groups also contributes to attract metal cations: the dual effect of amine group and oxime group explains the strong increase in sorption properties [71]. Under selected experimental conditions (low metal concentration) metal is

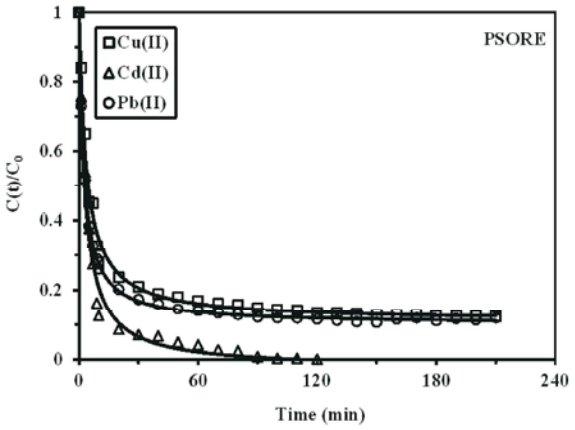

Fig. 4: Uptake kinetics – Modeling with the PSORE (SD: 1 g L^{-1}; C_0: 40 mg L^{-1}; pH 4 ± 0.1; agitation speed: 210 rpm, temperature: 25 ± 1 °C).

very efficiently removed from the solution at pH 4.4 for Pb(II), at pH 5.2 for Pb(II) and pH 5.7 for Cd(II): concentrations are below the detection limits.

For the sorption of metal cations such as Cd(II), Cu(II) and Zn(II), Anirudhan and Ramachandran [51]suggested that amidoxime acts as a bidentate ligand and proposed the interaction of two amidoxime groups from vicinal chains for the binding of one metal cation; they also observed a strong increase in sorption performance with the progressive deprotonation of the polymer up to pH 6 where the surface becomes negatively charged (pH_{ZPC} close to 6). Chen et al. [69]used XPS analysis for confirming the contribution of amine and hydroxyl groups on the binding of Cu(II) and Pb(II) on amidoximated bacterial cellulose.

Figure S6 (see Supplementary Material) shows the pH variation during metal binding. The three metal ions have roughly similar trends. At pH 1, the pH variation is negligible. In the pH range between 2 and 4, the pH of the solution tends to increase by up to 1-1.5 pH unit. At pH 5 and above for Cd(II) and Pb(II), the pH tends to stabilize around pH 5-5.5. This "buffering" effect is probably due to the deprotonation of oxime [73] and to the formation of hydrolyzed species. In the case of Cu(II), a little difference is observed: the trend to alkalinize the solution is prolonged till pH 6; above pH 6 the solutions tends to be acidified but the pH slightly increases (contrary to the stabilization observed with the other metal cations). This is probably associated to a higher sensitivity of Cu(II) to pH hydrolysis.Experimental conditions have been selected to avoid possible phenomena of metal precipitation; this was verified using MEDUSA[75] and Visual MINTEQ [76]speciation computing programs.

Uptake Kinetics: Figure 4 shows that metal sorption is fast under selected experimental conditions. After 10 min of contact more than 70 % of Cu(II) and Pb(II) are removed and up to 88 % of Cd(II) is recovered. After 90 min of contact more than 99 % of total sorption was achieved. This contact time was used for further experiments. The weak fraction of metal sorption after 10 min of contact means that the reactive groups are available and accessible and that mass transfer properties are weakly affected by the resistance to intraparticle diffusion. This is consistent with the structure observed by SEM (Figure S1, see Supplementary Material) and specific surface area measurements: interconnected macroporous network, surface microporosity and specific surface area (66-70 $m^2\ g^{-1}$) are favorable for fast sorption.

The modeling of uptake kinetics was tested using the PFORE (Figure S7, see Supplementary Material) and the PSORE (Figure 6). PSORE fits much better experimental data than PFORE (Table 1). The estimated variance (EV) and the determination coefficients are significantly lower with PSORE. The comparison of the sorption capacities at equilibrium for experiments ($q_{eq,exp.}$)and for calculated values ($q_{eq,1}$ and $q_{eq,2}$) shows that PSORE gives closer values to experimental data.Figure S7 also shows the Weber and Morris plots: two segments are identified. Most of the sorption occurs within the first 10 minutes of contact with a clear linear trend while the second part of the curves is characterized by a linear trend (with very low slope) that tends to confirm that the interconnected porosity of the material limits the effects of resistance to intraparticle diffusion.

The strict comparison of model parameters for the three metal cations is difficult since the initial concentration was set to 40 mg L^{-1} that corresponds to different molar concentrations (i.e., 0.629 mmol Cu L^{-1}, 0.356 mmol Cd L^{-1} and 0.193 mmol Pb L^{-1}). Obviously, increasing the molar concentration of the metal increases the sorption capacity at equilibrium. On the other hand, the apparent kinetic rate (k_2) varies reciprocally with the initial molar concentration of metal ions in the solution. The apparent rate coefficient k_2 varies between 0.49 and 2.41 g $mmol^{-1}\ min^{-1}$, this is a little lower than the values cited by Metwally et al. for the sorption of metal cations on amidoximated Ce(IV) phosphate/PAN sorbent [48].

Similar fast kinetics were reported for Cu(II) and Zn(II) binding using lignocellulosic-based sorbent grafted with amidoxime [66], Cu(II) binding on amidoxime-starch sorbent [70], Cu(II) and Pb(II) sorption on amidoximated bacterial cellulose [77]: the equilibrium was systematically reached with 2-3 hours of contact.

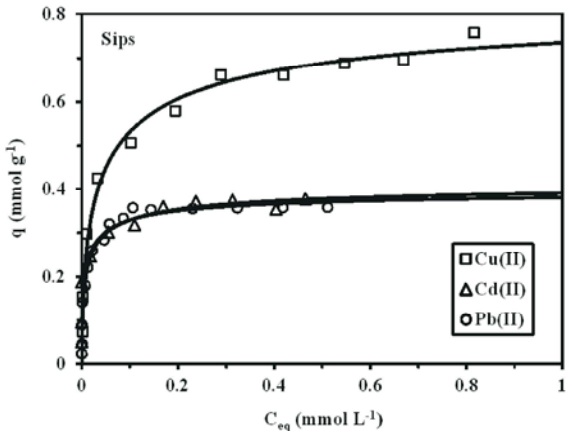

Fig. 5: Sorption isotherms – Modeling with the Sips equation (SD: 1 g L^{-1}; C_0: 5-100 mg L^{-1}; pH 4 ± 0.1; agitation time: 90 min, temperature: 25 ± 1 °C).

Sorption Isotherms: The sorption isotherms are reported on Figure 5. Lead and cadmium sorption are comparable (maximum sorption capacities in the range 0.36-0.38 mmol g^{-1}) and much lower than the sorption capacities reached with Cu(II) (around 0.76 mmol g^{-1}). The steepness of the initial slope of the curves indicates that the sorbent has a good affinity for metal ions. Three equations have been compared for the modeling of experimental profiles (Table S2, see Supplementary Material). The saturation plateau observed on Figure 5 means that the Langmuir-based models (i.e., Langmuir equation and Sips equation) are more appropriate for fitting experimental data than the power-type function of the Freundlich equation (Table 2). The lowest estimated variances and the highest determination coefficients are obtained with the Sips equation. This equation fits experimental data through the determination of 3 parameters contrary to the Langmuir and the Freundlich equations that are defined by only two parameters: the statistical approach is then better with the former equations. Obviously, introducing a supplementary parameter (as in the case of the Sips equation) improves the quality of mathematical fit of experimental data. However, this additional parameter has no physico-chemical significance and the equation should only be used for mathematically predicting sorption capacities.The superimposition of fitted curves to experimental points on Figure 5 confirms these conclusions while Figures S8 and S9 (see Supplementary Material) show some discrepancies in the fit of the curvature of the isotherm curve (Langmuir equation) or in the approach of material saturation (Freundlich).

The maximum sorption capacities can be affected by different parameters such as their hydrated ionic size and/or their softness. Indeed, according to the Pearson's rule (HSAB theory: hard and soft acid and base theory), hard acids (metal ions) will react preferentially and faster with hard bases (ligands) and reciprocally soft acids will readily bind to soft bases [78]. The softness parameters are 0.38, 0.41 and 0.58 for Cu(II), Pb(II) and Cd(II), respectively [79]. There is no correlation between the softness parameter and the maximum sorption capacities ($q_{m,exp}$) nor the affinity coefficient (b_L) (Table 2). The size of hydrated species also strongly impacts the reactivity of metal ions with given ligands. The ranking of hydrated ionic radius follows the sequence: Cu(II) (0.73 Å) < Cd(II) (0.95 Å) < Pb(II) (1.19 Å); this corresponds to the reciprocal trend in maximum sorption capacities: Cu(II) (0.758 mmol g^{-1}) > Cd(II) (0.378 mmol g^{-1}) > Pb(II) (0.358 mmol g^{-1}). Smaller ionic size for metal ion hydrated species facilitates the steric arrangement of the metal ion in the complex with amidoxime reactive groups.

The sorption properties of the sorbent for Cu(II), Cd(II) and Pb(II) were compared to sorption properties obtained with other conventional sorbents in Table S5 (see Supplementary Material). The table shows that this sorbent has a lower sorption than some other materials such as nanofibers [80]. However, compared to activated carbon or even some other amidoxine-based sorbents,this composite shows good sorption properties. It is noteworthy that the actual fraction of PAN/amidoxime compartment in the sorbent is limited to 50 %. This means that the effective sorption capacity of the organic fraction is doubled and nearer to the levels obtained with some of the other amidoxime-based sorbents.The interconnected porosity of the zeolite-based material is another advantage since the uptake kinetics are relatively fast.

Thermodynamic Parameters: In order to verify the impact of temperature on sorption performance, the sorption capacities were compared at different temperatures, under similar experimental conditions (not shown). Actually, the sorption capacities slightly increases with the temperature for Cu(II) and Cd(II) while it decreases for Pb(II): Cu(II) and Cd(II) binding is endothermic while Pb(II) is exothermic. In order to evaluate the thermodynamic parameters the logarithm of the distribution coefficient, K_d (L g^{-1}), which is calculated as the ratio: $K_d = q_{eq}/C_{eq}$, is plotted *vs.* the reciprocal of absolute temperature (van't Hoff equation):

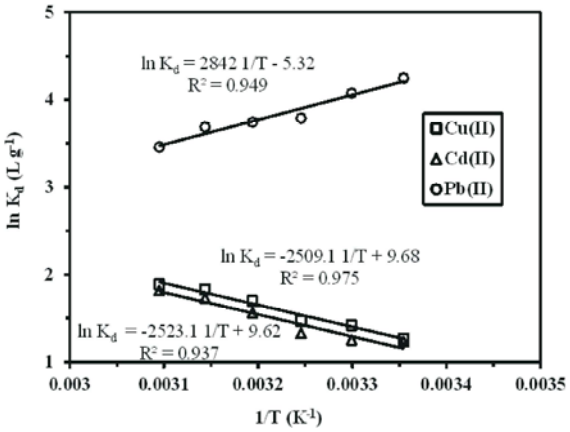

Fig. 6: Thermodynamics of metal sorption - Effect of temperature (K) on the distribution coefficient (K_d, L g^{-1}) (SD: 1 g L^{-1}; C_0: 40 mg L^{-1}; pH_0: 4 for Cu(II) and Cd(II) and pH_0: 4 for Pb(II); contact time: 90 min).

$$ln\ K_d = \frac{-\Delta H^o}{RT} + \frac{-\Delta S^o}{R} \quad (5a)$$

$$\Delta G^o = \Delta H^o - T\Delta S^o \quad (5b)$$

where ΔH^0 (kJ mol^{-1}) is the enthalpy change, ΔG^0 (kJ mol^{-1}) is the free energy change and ΔS^0 (J $mol^{-1}K^{-1}$) is the entropy change (R is the gas constant, 8.314 J mol^{-1} K^{-1}).

Figure 6 shows very similar thermodynamic profiles for Cu(II) and Cd(II) sorption while a reciprocal trend is observed for Pb(II) sorption. These data are used for calculating the thermodynamic constants (Table S6, see Supplementary Material). As expected the constant are very close for Cu(II) and Cd(II) sorption and completely opposed to those of Pb(II) sorption. The positive values of ΔH^0confirms that the sorption of Cu(II) and Cd(II) is endothermic contrary to Pb(II) binding. The positive value of the entropy change corresponds to an increase in the disorder of the system. This is sometimes explained by the release of water from hydrated form of the metal ion during metal binding. On the opposite hand, the negative value of entropy change for Pb(II) sorption means that the system is more organized after metal binding. The negative values of the Gibbs free energy indicate that the equilibrium constants are relatively higherfor Cu(II) and Cd(II) compared with the value for Pb(II). In the case of Cu(II) and Pb(II) sorption using amidoximated bacterial cellulose, the enthalpy, the entropy and the Gibbs free energy changes were all negative [77]. A completely different trend was reported by Metwally et al.[48]in the case of Ni(II), Pb(II) and Cd(II) using Ce(IV) phosphate/PAN functionalized with amidoxime.

Influence of the Composition of the Solution: The sorption properties may be strongly affected by the composition of the solution. In order to verify the effect of complex media on the binding of metal cations, the sorption efficiencies for Cu(II), Cd(II) and Pb(II) are compared in the presence of increasing concentrations of NaCl and humic acid (chosen as a simulate of soil extract, present in many surface waters)(Figures S10 and S11, see Supplementary Material, respectively). The presence of sodium chloride increases the ionic strength of the solution without affecting the efficiency of metal sorption: Na(I) has poor affinity for amidoxime groups and chloride ions are not strong ligands for target metal cations. As a consequence, the effect of NaCl addition is relatively limited. The impact of NaCl ionic strength would be more important for a process involving ion exchange properties; this is less marked for this chelation mechanism.

Humic acid (HA) is present in many water bodies as the result of the extraction of organic materials from soils [81]; it contains numerous carboxylic, amine, hydroxyl and phenolic groups that can be readily deprotonated in weakly acid or neutral solutions. Humic acid controls the redistribution of heavy metal ions between soil and hydrosphere [82]. Humic acid can bind metal cations by complexation mechanisms [83]; as a consequence metal ions may be less available for metal binding by the sorbent. Figure S11 (see Supplementary Material) confirms that the presence of low concentrations of humic acid (up to 20 mg HA L^{-1}) induces a progressive decrease in the sorption efficiency; however, above a concentration of 30 mg HA L^{-1}, the sorption efficiency slightly increases. At low metal concentration the soluble complexes formed between metal cations and humic acid limits the availability of metal cations, while at higher HA concentration the organic ligand may be partially bound to the sorbent contributing to additional metal sorption.

Influence of the Sorbent Dosage: The sorbent dosage was varied in order to evaluate the impact of this parameter on the optimal conditions for metal recovery (Figure S12, see Supplementary Material). As expected, increasing the sorbent dosage, for fixed metal concentrations, increases the sorption efficiencies and decreases the sorption capacities. Selecting optimal conditions in terms of sorbent dosage is then controlled

by the objective of the process. For environmental applications, with the objective of reducing as much as possible the residual concentration it is necessary increasing the sorbent dosage. For concentrations as high as 40-50 mg $L^{-1}$the sorption efficiencies tend to level offat a sorbent dosage of 1.6-2 g L^{-1} with residual concentrations ranging between 0.09 mg L^{-1} and 0.36 mg L^{-1}. Except for copper (standard limits: 2 mg L^{-1}) these values are higher than the standards accepted for WHO drinking waterstandards (i.e., 0.003 mg Cd L^{-1} and 0.01 mg Pb L^{-1}) [1] and for EU drinking water standards (i.e., 0.005 mg Cd L^{-1} and 0.01 mg Pb L^{-1})[84]. This means that the process will not be able to competitively treat effluents containing so high levels of concentrations: in this case the process should be considered as a pre-treatment. Lower initial concentrations would obviously change the conclusion. It is noteworthy that Cd(II) recovery is clearly less efficient in terms of environmental application than for Cu(II) and Pb(II), under selected experimental conditions.

When the objective of the treatment consists of metal recovery the target is to concentrate as much as possible the metal through the sorption/desorption operations and in this case it is better achieving high sorption capacities and sorbent dosage should be below 1 g L^{-1}. Under these conditions the sorption capacities are higher than 0.6 mmol Cu g^{-1}, 0.35 mmol Cd g^{-1} and 0.2 mmol Pb g^{-1}. After metal desorption (with appropriate selection of volume of eluent compared to the volume of solution to be treated) the concentration effect may justify metal valorization.

With initial metal concentrations in the range 40-50 mg L^{-1} an intermediary sorbent dosage (close to 1.2 g L^{-1}) offers a good compromise in terms of sorption capacity and uptake efficiency.

Metal Desorption and Sorbent Recycling: Several techniques exist for desorbing metal ions from metal-loaded sorbents,such as: (a) pH change [49, 70, 85], or (b) reaction with a strong complexing agent such as ethylenediaminetetraacetic acid [86]. The use of a strong ligand makes more complex the recovery of the metals from these complex eluates and acidic solutions are generally preferable. The strong effect of pH on metal binding (Figure 3) indicates that acidic solutions may reverse metal binding. Desorption of copper ions from loaded sorbent was tested using HCl solutions at different concentrations. Figure S13a (see Supplementary Material) shows the kinetic profiles for desorption of Cu(II) ions from loaded sorbent: as expected increasing acid concentration improves desorption efficiency and decreases the time required for the stabilization of desorption yield. The equilibrium of desorption is reached between 40 and 60 min. Desorption kinetics is little faster than uptake kinetics; where 90min are necessary for reaching the equilibrium (Figure 4). The minimal concentration of HCl for achieving good metal desorption (i.e.; higher than 94%) is 0.5 M; increasing acid concentration above 0.5 M does not significantly improve metal recovery from the sorbent. Figure S13b (see Supplementary Material) illustrates the sorption performance of the sorbent when re-used after desorption step.; An intermediary rinsing step with demineralized water is intercalated between sorption and desorption steps. The sorption capacity is compared to the sorption capacity at initial stage for calculating the regeneration efficiency (RE, %). The kinetic profiles for the test of regeneration properties are also influenced by the concentration of HCl. For the samples desorbed with low HCl concentration solutions, the kinetics is relative slow requiring 60 min of contact; on the opposite hand, for higher HCl concentrations, 40 minutes of contact are generally sufficient. For the samples desorbed under the most favorable conditions (i.e., 0.5 M and 0.6 M HCl solutions) the regeneration efficiency was higher than 94%. A concentration of HCl close to 0.5 M is selected for further experiments on other metal ions.

The desorption percentages are 94.2%, 92.2 % and 89.2% for Cu(II), Cd(II) and Pb(II). The next sorption step shows that sorption capacity remain close to the levels reached at the first step: the regeneration efficiencies are 93.6%, 89.4 % and 88.3 % for Cu(II), Cd(II) and Pb(II), respectively. This slight decrease in sorption performance is consistent with the progressive decrease in sorption efficiency observed for other similar sorbents [70, 87]. Similar trends were observed under similar conditions for Cd(II) desorption (Figure S14, see Supplementary Material) and for Pb(II) desorption (Figure S15, see Supplementary Material).

Table 3 reports the sorption and desorption performances for the recovery of Cu(II), Cd(II) and Pb(II) for 5 successive sorption/desorption cycles.The efficiencies of desorption nand regeneration are remarkably stable. Though a little decrease is observed between the first and the last cycles, this decrease does not exceed 4-5 %, regardless of the metal ion. These results confirm the possibility to re-use the sorbent for a minimum of 5 cycles.

Application to the Purification of Local Tap Water: In order to evaluate the potential of this sorbent for the recovery of these heavy metals from real-like effluents and for testing the possibility to use this material for water

purification a tap water delivered by the local water supply company (Damietta Water Company, Egypt) was spiked with Cu(II), Cd(II) and Pb(II) at two levels of metal concentration (i.e., around 3 mg L^{-1} and around 4-5 mg L^{-1}) (Table 5).

The removal efficiencies range between 80 % and 88 % with residual concentrations ranging between 0.3 mg L^{-1} and 1 mg L^{-1}; this means that the decrease in metal concentrations is not sufficient for reaching water drinking standards, except for Cu(II). Higher sorbent dosage would be necessary for achieving target values. This also means that the process could probably be used for the treatment of individual water supply (for example as a cartridge unit plugged on water entry) point rather than for the treatment of water supply network. The sorption capacities are relatively low, as expected due to the low level of metal concentrations.

CONCLUSION

This study clearly shows that the simple preparation of this composite material, produced by coating of polyacrylonitrile (through polymerization reaction) on Na-Y-zeolite and further functionalized by conversion of nitrile groups into amidoxime groups, is performant for synthesizing an efficient sorbent. FTIR analysis confirms the successful functionalization of PAN/Na-Y-zeolite. The sorbent effectively binds Cu(II), Cd(II) and Pb(II) in weakly acidic to neutral solutions (pH higher than 4). The binding reaction takes place on oxime and amine groups and is improved by pH increase (due to deprotonation of amine groups). The uptake kinetics are well described by the pseudo-second order rate equation while sorption isotherms are fitted by the Sips equation. Surprisingly, despite similar sorption mechanisms, the thermodynamic parameters are substantially different for Cu(II) and Cd(II) (sorption is endothermic and characterized by positive entropy) and for Pb(II) (exothermic sorption with negative entropy); no explanation was found to this thermodynamic "inversion". The presence of NaCl does not significantly change sorption performance (in the range 10-60 mg L^{-1}) while humic acid slightly reduces sorption performance, due to the complexation of metal ions that are less available for binding on amidoxime groups of the sorbent. Acidic solutions (0.5 M HCl) are efficient for metal desorption and sorbent recycling: sorption and desorption properties remain stable for a minimum of 5 cycles of sorption/desorption.

This simple-to-prepare sorbent, based on the use of abundant zeolite support, appears a promising material for the recovery of heavy metal ions. In the treatment of spiked tap water the process does not achieved standard levels for drinking water for Cd(II) and Pb(II), requiring higher sorbent dosages. This means that the sorbent could be used as fixed-bed cartridge for the purification of individual water supply points rather than for large scale units for production of drinking water.

Recent advances have shown that multi-functional groups containing complementary vicinal reactive groups such as DETA and phosphorylated amine groups may improve sorption selectivity, even in complex media such as seawater [46]. This is part of the strategy that could be used for improving metal sorption properties of the present composite material.

ACKNOWLEDGEMENTS

Authors thank Professor M.A. Diab for contributing to analysis and characterization.

REFERENCES

1. WHO, Guidelines for drinking-water quality, 4th Ed. ed., World Health Organization, Geneva (Switzerland), 2011.
2. Azimi, S. and V. Rocher, 2016. Influence of the water quality improvement on fish population in the Seine River (Paris, France) over the 1990-2013 period, Sci. Total Environ., 542: 955-964.
3. Monroy, M., A. Maceda-Veiga and A. de Sostoa, 2014. Metal concentration in water, sediment and four fish species from Lake Titicaca reveals a large-scale environmental concern, Sci. Total Environ., 487: 233-244.
4. Tchounwou, P.B., C.G. Yedjou, A.K. Patlolla and D.J. Sutton, 2012. Heavy metals toxicity and the environment, in: A. Luch (Ed.) Molecular, Clinical and Environmental Toxicology, Springer, Basel (Switzerland), pp: 133-164.
5. Yolcubal, I., A.D. Demiray, E. Ciftci and E. Sangu, 2016. Environmental impact of mining activities on surface water and sediment qualities around Murgul copper mine, Northeastern Turkey, Environ. Earth Sci., pp: 75.
6. Beane, S.J., S.D.W. Comber, J. Rieuwerts and P. Long, 2016. Abandoned metal mines and their impact on receiving waters: A case study from Southwest England, Chemosphere, 153 (2016) 294-306.

7. Chauhan, D., M. Jaiswal and N. Sankararamakrishnan, 2012. Removal of cadmium and hexavalent chromium from electroplating waste water using thiocarbamoyl chitosan, Carbohydr. Polym., 88: 670-675.
8. Islamoglu, S., L. Yilmaz and H.O. Ozbelge, 2006. Development of a precipitation based separation scheme for selective removal and recovery of heavy metals from cadmium rich electroplating industry effluents, Sep. Sci. Technol., 41: 3367-3385.
9. Paulino, A.T., L.B. Santos and J. Nozaki, 2008. Removal of Pb^{2+}, Cu^{2+} and Fe^{3+} from battery manufacture wastewater by chitosan produced from silkworm chrysalides as a low-cost adsorbent, React. Funct. Polym., 68: 634-642.
10. Prado, A.G.S., A.O. Moura, M.S. Holanda, T.O. Carvalho, R.D.A. Andrade, I.C. Pescara, A.H.A. de Oliveira, E.Y.A. Okino, T.C.M. Pastore, D.J. Silva and L.F. Zara, 2010. Thermodynamic aspects of the Pb adsorption using Brazilian sawdust samples: Removal of metal ions from battery industry wastewater, Chem. Eng. J., 160: 549-555.
11. Vergili, I., Z.B. Gonder, Y. Kaya, G. Gurdag and S. Cavus, 2017. Sorption of Pb (II) from battery industry wastewater using a weak acid cation exchange resin, Process Saf. Environ. Prot., 107: 498-507.
12. Marani, D., J.W. Patterson and P.R. Anderson, 1995. Alkaline precipitation and aging of Cu(II) in the presence of sulfate, Water Res., 29: 1317-1326.
13. Jha, M.K., D. Gupta, P.K. Choubey, V. Kumar, J. Jeong and J.C. Lee, 2014. Solvent extraction of copper, zinc, cadmium and nickel from sulfate solution in mixer settler unit (MSU), Sep. Purif. Technol., 122: 119-127.
14. Ochromowicz, K. and T. Chmielewski, 2013. Solvent extraction of copper(II) from concentrated leach liquors, Physicochem. Prob. Miner. Process., 49: 357-367.
15. Gonzalez, M.P., I. Saucedo, R. Navarro, M. Avila and E. Guibal, 2001. Selective separation of Fe(III), Cd(II) and Ni(II) from dilute solutions using solvent-impregnated resins, Ind. Eng. Chem. Res., 40: 6004-6013.
16. Arias, A., I. Saucedo, R. Navarro, V. Gallardo, M. Martinez and E. Guibal, 2011. Cadmium(II) recovery from hydrochloric acid solutions using Amberlite XAD-7 impregnated with a tetraalkyl phosphonium ionic liquid, React. Funct. Polym., 71; 1059-1070.
17. Kica, M., T. Vincent, A. Trochimczuk, R. Navarro and E. Guibal, 2014. Tetraalkylphosphonium ionic liquid encapsulation in alginate beads for Cd(II) sorption from HCl solutions, Solvent Extr. Ion Exch., 32: 543-561.
18. Ahmed, I.A.M., S.D. Young and N.M.J. Crout, 2010. Ageing and structural effects on the sorption characteristics of Cd^{2+} by clinoptilolite and Y-type zeolite studied using isotope exchange technique, J. Hazard. Mater., 184: 574-584.
19. Kim, J.S. and M.A. Keane, 2000. Ion exchange of divalent cobalt and iron with Na-Y zeolite: Binary and ternary exchange equilibria, J. Colloid Interface Sci., 232: 126-132.
20. Gonzalez, M.A., I. Pavlovic and C. Barriga, 2015. Cu(II), Pb(II) and Cd(II) sorption on different layered double hydroxides. A kinetic and thermodynamic study and competing factors, Chem. Eng. J., 269: 221-228.
21. Alslaibi, T.M., I. Abustan, M.A. Ahmad and A. Abu Foul, 2014. Kinetics and equilibrium adsorption of iron (II), lead (II) and copper (II) onto activated carbon prepared from olive stone waste, Desalin. Water Treat., 52: 7887-7897.
22. Prado Cechinel, M.A., S.M.A. Guelli Ulson de Souza and A.A. Ulson de Souza, 2014. Study of lead (II) adsorption onto activated carbon originating from cow bone, J. Cleaner Prod., 65: 342-349.
23. Gujar, R.B. and P.K. Mohapatra, 2015. Amazing selectivity for Am(III) uptake by composite graphene oxide-PES polymeric beads prepared by phase inversion, RSC Adv., 5: 24705-24711.
24. Guibal, E., 2004. Interactions of metal ions with chitosan-based sorbents: a review, Sep. Purif. Technol., 38: 43-74.
25. Farooq, U., J.A. Kozinski, M.A. Khan and M. Athar, 2010. Biosorption of heavy metal ions using wheat based biosorbents - A review of the recent literature, Bioresour. Technol., 101: 5043-5053.
26. Bhatnagar, A., V.J.P. Vilar, C.M.S. Botelho and R.A.R. Boaventura, 2010. Coconut-based biosorbents for water treatment - A review of the recent literature, Adv. Colloid Interface Sci., 160: 1-15.
27. Bulgariu, D. and L. Bulgariu, 2016. Potential use of alkaline treated algae waste biomass as sustainable biosorbent for clean recovery of cadmium(II) from aqueous media: batch and column studies, J. Cleaner Prod., 112: 4525-4533.

28. Yargic, A.S., R.Z.Y. Sahin, N. Ozbay and E. Onal, 2015. Assessment of toxic copper(II) biosorption from aqueous solution by chemically-treated tomato waste, J. Cleaner Prod., 88 (2015) 152-159.
29. Erdem, E., N. Karapinar and R. Donat, 2004. The removal of heavy metal cations by natural zeolites, J. Colloid Interface Sci., 280: 309-314.
30. Lutz, W. and Y. Zeolite, 2014. Synthesis, modification and properties-A Case revisited, Adv. Mater. Sci. Eng., (2014).
31. Faghihian, H., M. Iravani, M. Moayed and M. Ghannadi-Maragheh, 2013. Preparation of a novel PAN-zeolite nanocomposite for removal of Cs^{+} and Sr^{2+} from aqueous solutions: Kinetic, equilibrium and thermodynamic studies, Chem. Eng. J., 222: 41-48.
32. Kaygun, A.K. and S. Akyil, 2007. Study of the behaviour of thoriurn adsorption on PAN/zeolite composite adsorbent, J. Hazard. Mater., 147: 357-362.
33. Akl, Z.F., S.M. El-Saeed and A.M. Atta, 2016. In-situ synthesis of magnetite acrylamide amino-amidoxime nanocomposite adsorbent for highly efficient sorption of U(VI) ions, J. Ind. Eng. Chem., 34: 105-116.
34. Horzum, N., T. Shahwan, O. Parlak and M.M. Demir, 2012. Synthesis of amidoximated polyacrylonitrile fibers and its application for sorption of aqueous uranyl ions under continuous flow, Chem. Eng. J., 213: 41-49.
35. Mahdavinia, G.R. and E. Shokri, 2017. Synthesis and characterization of magnetic amidoximated chitosan-g poly (polyacrylonitrile)/laponite RD nanocomposites with enhanced adsorption capacity for Cu^{2+}, Turk. J. Chem., 41: 135-152.
36. Bayramoglu, G. and M.Y. Arica, 2016. MCM-41 silica particles grafted with polyacrylonitrile: Modification in to amidoxime and carboxyl groups for enhanced uranium removal from aqueous medium, Microporous Mesoporous Mater., 226: 117-124.
37. Bayramoglu, G., A. Akbulut and M.Y. Arica, 2015. Study of polyethyleneimine- and amidoxime-functionalized hybrid biomass of Spirulina (Arthrospira) platensis for adsorption of uranium (VI) ion, Environ. Sci. Pollut. Res., 22: 17998-18010.
38. Wang, Y., Z.X. Gu, J.J. Yang, J.L. Liao, Y.Y. Yang, N. Liu and J. Tang, 2014. Amidoxime-grafted multiwalled carbon nanotubes by plasma techniques for efficient removal of uranium(VI), Appl. Surf. Sci., 320: 10-20.
39. Ramachandhran, V., S.C. Kumar and M. Sudarsanan, 2001. Preparation, characterization and performance evaluation of styrene-acrylonitrile-amidoxime sorbent for uranium recovery from dilute solutions, J. Macromol. Sci. Part A Pure Appl. Chem., 38: 1151-1166.
40. Saito, T., S. Brown, S. Chatterjee, J. Kim, C. Tsouris, R.T. Mayes, L.J. Kuo, G. Gill, Y. Oyola, C.J. Janke and S. Dai, 2014. Uranium recovery from seawater: development of fiber adsorbents prepared via atom-transfer radical polymerization, J. Mater. Chem. A, 2: 14674-14681.
41. Kim, J., C. Tsouris, Y. Oyola, C.J. Janke, R.T. Mayes, S. Dai, G. Gill, L.J. Kuo, J. Wood, K.Y. Choe, E. Schneider and H. Lindner, 2014. Uptake of uranium from seawater by amidoxime-based polymeric adsorbent: field experiments, modeling and updated economic assessment, Ind. Eng. Chem. Res., 53 (2014) 6076-6083.
42. Kim, J., Y. Oyola, C. Tsouris, C.R. Hexel, R.T. Mayes, C.J. Janke and S. Dai, 2013. Characterization of uranium uptake kinetics from seawater in batch and flow-through experiments, Ind. Eng. Chem. Res., 52: 9433-9440.
43. Oyola, Y. and S. Dai, 2016. High surface-area amidoxime-based polymer fibers co-grafted with various acid monomers yielding increased adsorption capacity for the extraction of uranium from seawater, Dalton Trans., 45: 8824-8834.
44. Zeng, Z.H., Y.Q. Wei, L. Shen and D.B. Hua, 2015. Cationically charged poly(amidoxime)-grafted polypropylene nonwoven fabric for potential uranium extraction from seawater, Ind. Eng. Chem. Res., 54: 8699-8705.
45. Guo, X., L. Huang, C. Li, J. Hu, G. Wu and P. Huai, 2015. Sequestering uranium from $UO_2(CO_3)(_3)(^{4-})$ in seawater with amine ligands: density functional theory calculations, Phys. Chem. Chem. Phys., 17: 14662-14673.
46. Alexandratos, S.D., X.P. Zhu, M. Florent and R. Sellin, Polymer-supported bifunctional amidoximes for the sorption of uranium from seawater, Ind. Eng. Chem. Res., 55: 4208-4216.
47. Ajmal, M., S. Demirci, M. Siddiq, N. Aktas and N. Sahiner, 2016. Amidoximated poly(acrylonitrile) particles for environmental applications: Removal of heavy metal ions, dyes and herbicides from water with different sources, J. Appl. Polym. Sci., pp: 133.

48. Metwally, S.S., R.R. Ayoub and H.F. Aly, 2013. Amidoximation of cyano group for chelating ion exchange of some heavy metal ions from wastewater, Sep. Sci. Technol., 48: 1829-1839.
49. Abdel-Razik, H.H. and E.R. Kenawy, 2012. Synthesis, characterization and amidoximation of diaminomaleodinitrile-functionalized polyethylene terephthalate grafts for collecting heavy metals from wastewater, J. Appl. Polym. Sci., 125: 1136-1145.
50. Mun, S.P., C.S. Ku and J.P. Kim, 2010. Adsorption of metal and uranyl ions onto amidoximated Pinus densiflora bark, Wood Sci. Technol., 44: 283-299.
51. Anirudhan, T.S. and M. Ramachandran, 2008. Synthesis and characterization of amidoximated polyacrylonitrile/organobentonite composite for Cu(II), Zn(II) and Cd(II) adsorption from aqueous solutions and industry wastewaters, Ind. Eng. Chem. Res., 47: 6175-6184.
52. Lutfor, M.R. and M.Y. Mashitah, 2011. Synthesis of poly(hydroxamic acid)-poly(amidoxime) chelating ligands for removal of metals from industrial wastewater, E-J. Chem., 8: 1038-1043.
53. Lutfor, M.R., S. Silong, W.M. Zin, M.Z. Ab Rahman, M. Ahmad and J. Haron, 2000. Preparation and characterization of poly(amidoxime) chelating resin from polyacrylonitrile grafted sago starch, Eur. Polym. J., 36: 2105-2113.
54. Tien, C., 1994. Adsorption Calculations and Modeling, Butterworth-Heinemann, Newton, MA.
55. Ho, Y.S. and G. McKay, 1999. Pseudo-second order model for sorption processes, Process Biochem., 34: 451-465.
56. Lagergren, S., 1898. About the theory of so-called adsorption of soluble substances., Kungliga Swenska Vet., 24: 1-39.
57. Weber, W.J. and J.C. Morris, 1963. Kinetics of adsorption on carbon from solutions., J. Sanitary Eng. Div., ASCE, 89: 31-60..
58. Langmuir, I., 1918. The adsorption of gases on plane surfaces of glass, mica and platinum, J. Amer. Chem. Soc., 40: 1361-1402.
59. Freundlich, H.M.F., 1906. Uber die adsorption in lasungen, Z. Phys. Chem., 57: 385-470.
60. Jiao, W.Q., W.H. Fu, X.M. Liang, Y.M. Wang and M.Y. He, 2014. Preparation of hierarchically structured Y zeolite with low Si/Al ratio and its applications in acetalization reactions, RSC Adv., 4: 58596-58607.
61. Barik, S., L. Behera and S.K. Badamali, 2017. Assessment of thermal and antimicrobial properties of PAN/Zn-Al layered double hydroxide nanocomposites, Compos. Interfaces, 24: 579-591.
62. Zahri, N.A.M., S. Jamil, L.C. Abdullah, T.C.S. Yaw, M.N. Mobarekeh, S.J. Huey and N.S.M. Rapeia, 2015. Improved method for preparation of amidoxime modified poly(acrylonitrile-co-acrylic acid): Characterizations and adsorption case study, Polymers, 7: 1205-1220.
63. Sang, S.Y., Z.M. Liu, P. Tian, Z.Y. Liu, L.H. Qu and Y.Y. Zhang, 2006. Synthesis of small crystals zeolite NaY, Mater. Lett., 60; 1131-1133.
64. Moosavifar, M., S. Tangestaninejad, M. Moghadam, V. Mirkhani and I. Mohammadpoor-Baltork, 2013. Host (nanocavity of zeolite Y)-guest (ruthenium(III) salophen complex) nanocomposite materials: An efficient and reusable catalyst for shape-selective epoxidation of linear alkenes with sodium periodate, J. Mol. Catal. A: Chem., 377: 92-101.
65. Vivero-Escoto, J.L., M. Carboni, C.W. Abney, K.E. deKrafft and W. Lin, 2013. Organo-functionalized mesoporous silicas for efficient uranium extraction, Microporous Mesoporous Mater., 180: 22-31.
66. Anirudhan, T.S., L. Divya, C.D. Bringle and P.S. Suchithra, 2010. Removal of copper(II) and zinc(II) from aqueous solutions using a lignocellulosic-based polymeric adsorbent containing amidoxime chelating functional groups, Sep. Sci. Technol., 45: 2383-2393.
67. Ji, C.N., R.J. Qu, H. Chen, X.G. Liu, C.M. Sun and C.X. Ma, 2016. Hg(II) adsorption using amidoximated porous acrylonitrile/itaconic copolymers prepared by suspended emulsion polymerization, Water Sci. Technol., 73: 1709-1718.
68. Deng, S., G. Zhang, Y. Li, Y. Dou and P. Wang, 2016. Facile preparation of amidoxime-functionalized fiber by microwave-assisted method for the enhanced adsorption of chromium(VI) from aqueous solution, RSC Adv., 6: 64665-64675.
69. Chen, S., W. Shen, F. Yu, W. Hu and H. Wang, 2010. Preparation of amidoximated bacterial cellulose and its adsorption mechanism for Cu^{2+} and Pb^{2+}, J. Appl. Polym. Sci., 117: 8-15..
70. Dragan, E.S., D.F.A. Loghin and A.I. Cocarta, 2014. Efficient sorption of Cu^{2+} by composite chelating sorbents based on potato starch-graft-polyamidoxime embedded in chitosan beads, ACS Appl. Mater. Interfaces, 6: 16577-16592.

71. Kondo, K., M. Matsumoto and K. Okamoto, 1999. Enhanced adsorption of copper(II) ion on novel amidoxime chitosan resin, J. Chem. Eng. Jpn., 32: 217-222.
72. Nibel, O., M. Bon, M.L. Agiorgousis, T. Laino, L. Gubler and T.J. Schmidt, 2017. Unraveling the interaction mechanism between amidoxime groups and vanadium ions at various pH conditions, J. Phys. Chem. C, 121: 6436-6445.
73. Zhao, Z., X.H. Li, Y.Q. Chai, Z.S. Hua, Y.P. Xiao and Y.X. Yang, 2016. Adsorption performances and mechanisms of amidoxime resin toward gallium(III) and vanadium(V) from Bayer liquor, ACS Sustainable Chem. Eng., 4: 53-59.
74. Zhao, Y.G., J.X. Li, S.W. Zhang and X.K. Wang, 2014. Amidoxime-functionalized magnetic mesoporous silica for selective sorption of U(VI), RSC Adv., 4: 32710-32717.
75. Puigdomenech, I., 2010. MEDUSA (Make equilibrium diagrams using sophisticated algorithms), in, Royal Institute of Technology, Stockholm, Sweden, 2010.
76. Gustafsson, J.P., 2013. Visual MINTEQ, ver. 3.1, in, KTH, Royal Institute of Technology, (url: https://vminteq.lwr.kth.se/; accessed May 2017), Stockholm, Sweden, 2013.
77. Chen, S.Y., W. Shen, F. Yu and H.P. Wang, 2009. Kinetic and thermodynamic studies of adsorption of Cu^{2+} and Pb^{2+} onto amidoximated bacterial cellulose, Polym. Bull., 63: 283-297.
78. Pearson, R.G., 14966. Acids and bases, Science (New York, N.Y.), 151: 172-177.
79. Marcus, Y., 1997. Ion Properties, Marcel Dekker, Inc., New York, NY, 1997.
80. Cai, Z., J. Jia, Q. Zhang and H. Yang, 2015. Preparation of amidoxime surface-functionalized polyindole (ASFPI) nanofibers for Pb(II) and Cd(II) adsorption from aqueous solutions, RSC Adv., 5: 82310-82323.
81. Rodríguez-Murillo, J.C., G. Almendros and H. Knicker, 2017. Humic acid composition and humification processes in wetland soils of a Mediterranean semiarid wetland, J Soils Sediments, in press; doi: 10.1007/s11368-017-1663-y (2017).
82. Matsuda, M., A. Kaminaga, K. Hayakawa, N. Takisawa and T. Miyajima, 2009. Surfactant binding by humic acids in the presence of divalent metal salts, Colloids Surf., A, 347: 45-49.
83. Xu, J., W. Tan, J. Xiong, M. Wang, L. Fang and L.K. Koopal, 2016. Copper binding to soil fulvic and humic acids: NICA-Donnan modeling and conditional affinity spectra, J. Colloid Interface Sci., 473: 141-151.
84. EU, Council Directive 98/83/EC of 3 November 1998 on the quality of water intented for human consumption, in: E. Union (Ed.) Document 31998L0083, European Union, Brussels (Belgium), 1998.
85. Rahman, M.L., S.M. Sarkar, M.M. Yusoff, A.K.D. Kulkarni, Z.Z. Chowdhury and M.E. Ali, 2016. Poly(amidoxime) from polymer-grafted Khaya cellulose: An excellent medium for the removal of transition metal cations from aqueous solution, Bioresources, 11: 6780-6800.
86. Saliba, R., H. Gauthier, R. Gauthier and M. Petit-Ramel, 2000. Adsorption of copper(II) and chromium(III) ions onto amidoximated cellulose, J. Appl. Polym. Sci., 75: 1624-1631.
87. Rahman, M.L., S.M. Sarkar, M.M. Yusoff and M.H. Abdullah, 2016. Efficient removal of transition metal ions using poly(amidoxime) ligand from polymer grafted kenaf cellulose, RSC Adv., 6: 745-757.
88. Ahmad Rafiqi, F. and K. Majid, 2015. Removal of copper from aqueous solution using polyaniline and polyaniline/ferricyanide composite, J. Environ. Chem. Eng., 3: 2492-2501.
89. Mamun, A.A., 2016. Removal of cadmium from water by CNT–PAC composite: Effect of functionalization, Nano, 11: 95-101.
90. Huang, Y. and A.A. Keller, 2015. EDTA functionalized magnetic nanoparticle sorbents for cadmium and lead contaminated water treatment, Water Res., 80: 159-168.
91. Alothman, Z.A. and A.W. Apblett, 2010. Metal ion adsorption using polyamine-functionalized mesoporous materials prepared from bromopropyl-functionalized mesoporous silica, J. Hazard. Mater., 182: 581-590.
92. Khan, A., S. Badshah and C. Airoldi, 2011. Biosorption of some toxic metal ions by chitosan modified with glycidylmethacrylate and diethylenetriamine, Chem. Eng. J., 171: 159-166.
93. Coskun, R. and C. Soykan, 2009. Preparation of amidoximated polyester fiber and competitive adsorption of some heavy metal ions from aqueous solution onto this fiber, J. Appl. Polym. Sci., 112: 1798-1807.

94. Barakat, M.A. and R. Kumar, 2015. Synthesis and characterization of porous magnetic silica composite for the removal of heavy metals from aqueous solution, J. Ind. Eng. Chem., 23: 93-99.
95. Chung, S.G., J.C. Ryu, M.K. Song, B. An, S.B. Kim, S.H. Lee and J.W. Choi,2014. Modified composites based on mesostructured iron oxyhydroxide and synthetic minerals: A potential material for the treatment of various toxic heavy metals and its toxicity, J. Hazard. Mater., 267: 161-168.
96. Song, Y., J. Li, G. Ye, J. Xu and M. Jiang, 2015. Polyamidoxime/poly(vinyl alcohol) composite chelating fiber prepared by emulsion spinning and its adsorption properties for metal ions, Ind. Eng. Chem. Res., 54: 12367-12373.
97. Kampalanonwat, P. and P. Supaphol, 2010. Preparation and adsorption behavior of aminated electrospun polyacrylonitrile nanofiber mats for heavy metal ion removal, ACS Appl. Mater. Interfaces, 2: 3619-3627.